Quasiphase Transition in a Single File of Water Molecules Encapsulated in (6,5) Carbon Nanotubes Observed by Temperature-Dependent Photoluminescence Spectroscopy

Xuedan Ma,[1,*,‡] Sofie Cambré,[2,†] Wim Wenseleers,[2] Stephen K. Doorn,[1] and Han Htoon[1]
[1]Center for Integrated Nanotechnologies, Materials Physics and Applications Division, Los Alamos National Laboratory, New Mexico 87545, USA
[2]Experimental Condensed Matter Physics Laboratory, University of Antwerp, B-2610 Antwerp, Belgium
(Received 1 May 2016; published 12 January 2017)

Molecules confined inside single-walled carbon nanotubes (SWCNTs) behave quite differently from their bulk analogues. In this Letter we present temperature-dependent (4.2 K up to room temperature) photoluminescence (PL) spectra of water-filled and empty single-chirality (6,5) SWCNTs. Superimposed on a linear temperature-dependent PL spectral shift of the empty SWCNTs, an additional stepwise PL spectral shift of the water-filled SWCNTs is observed at ~150 K. With the empty SWCNTs serving as an ideal reference system, we assign this shift to temperature-induced changes occurring in the single-file chain of water molecules encapsulated in the tubes. Our molecular dynamics simulations further support the occurrence of a quasiphase transition of the orientational order of the water dipoles in the single-file chain.

DOI: 10.1103/PhysRevLett.118.027402

Confinement of molecules determines the properties and functions of many systems in biology, geology, catalysis, and nanofluidics [1]; e.g., nanoconfined water plays a vital role in selective single-file water and ion transport through biological membranes [2,3] and allows for the development of ultraselective nanofluidics applications [4–9]. Single-walled carbon nanotubes (SWCNTs) [10] are an excellent model system to study nanoconfined water due to their close analogy with many natural systems [11,12]. Additionally, they combine atomically precise diameters matching the size of various molecules with a one-dimensional character and possess structure-dependent optical properties that are extremely sensitive to the presence of encapsulated molecules, leading to characteristic spectral shifts [13–17]. In this Letter, we therefore exploit these optical transitions as ultrasenstive probes for the temperature-dependent behavior of a single file of water molecules encapsulated inside (6,5) SWCNTs. Molecular confinement inside SWCNTs moreover results in new functionalities such as amphoteric doping [18] or photosensitization [19,20] of the SWCNTs, enhanced stabilities of the encapsulated molecules [21], and unique molecular order, which is only achievable in such quasi-1D nanocavities [16]. Moreover, recent studies [5,22,23] have revealed nearly zero friction for confined water transportation and superior water permeability in carbon nanotubes, indicating their potential applications in efficient desalination and water purification devices [24,25].

Both theoretical calculations [4,26] and experiments [13–15,27,28] have demonstrated that water molecules can spontaneously enter the smooth, hydrophobic channels of SWCNTs. Remarkably, considering that Ising [29] already showed generally that long range (i.e., infinite range) order and thus a strict phase transition cannot exist in a 1D system with short-range interactions, theoretical simulations have predicted highly ordered structures of water confined inside SWCNTs, critically dependent on the tube diameter and chirality, and that additional changes between such structures may still occur [26,30,31]. As mathematically such changes cannot be strictly discontinuous, but clearly recognizable as a step (where the actual degree of rounding may still depend strongly on the dimensions of the system), we refer to these as quasiphase transitions. For SWCNTs with diameters $d \gtrsim 0.9$ nm, theory has predicted that confined water can transform into low-dimensional ice nanotubes, either continuously (unlike bulk water) or through a seemingly discontinuous (quasi-first-order) transition, with the freezing point being critically dependent on the SWCNT diameter (ranging from 150 up to 290 K) [26,31]. X-ray diffraction [32,33], infrared spectroscopy [34,35], neutron scattering [36], and nuclear magnetic resonance [37] studies have demonstrated the existence of such ice nanotubes. These experiments were however always performed on larger diameter samples with mixed chiralities and diameters (and using techniques unselective for the SWCNT diameter), thus providing only an average view on the water structure and phase transition over the entire diameter range.

Even more intriguing is the behavior of water in the smallest, yet fillable SWCNTs ($0.54 \leq d < 0.9$ nm [14]) where mutual passage of molecules is excluded and water molecules form one-dimensional single-file chains [30,38]. Quantum chemical calculations of water confined in these narrow diameters predict the existence of different ferroelectric ground state conformations, depending on the model used: the water dipoles, all pointing in the same

sense, either form an alternating, sizable angle with the SWCNT axis (classical hydrogen-bonded chains) [30,38,39], or are aligned parallel to the SWCNT axis (bifurcated hydrogen bonds) [14,40]. Although the restricted lateral mobility in a single file precludes distinguishing liquid from solid phases, [41] a transition in the orientational order of the water molecules cannot be excluded, for which experimental evidence is still lacking.

Recent advances in chiral sorting of carbon nanotubes [42–44], combined with the extreme sensitivity (and chiral selectivity [45]) of optical spectroscopy for the filling of SWCNTs with various molecules [13–16], provides an ideal platform for studying the thermodynamic properties of single files of water molecules confined in SWCNTs with a well-defined, small diameter. In this Letter, we report temperature-dependent photoluminescence (PL) spectroscopy of empty and water-filled sorted, single-chirality (6,5) SWCNTs. Superimposed on the linear shift of the emission energy of the empty SWCNTs, the PL of the water-filled SWCNTs shifts significantly at about 150 K, which is attributed to a change of the dipole orientations of the encapsulated water molecules. Molecular dynamics (MD) calculations indeed show that qualitative changes in orientational order should occur within the measured temperature range.

For the temperature-dependent PL experiments, a home-built confocal laser microscope was used (see also the Supplemental Material [46]). Samples were prepared as follows. An aqueous dispersion of SWCNTs produced by the high-pressure CO conversion method (HiPco) was prepared using sodium deoxycholate (DOC, 1 wt%/V) as surfactant by gentle magnetic stirring for 3 weeks. Sonication was avoided to prevent structural damage to the SWCNTs [13,57]. From this suspension, (6,5) SWCNTs were extracted by a two-step aqueous two-phase procedure [43,44]. The resulting chirality sorted nanotube suspension was first dialyzed to 1 wt%/V DOC, using a stirred ultrafiltration cell, and subsequently density gradient ultracentrifugation was used to separate the empty and water-filled (6,5) SWCNTs [58,59]. Similar to previous work [13–16,58,59] a combination of optical absorption, resonant Raman, and PL-excitation spectroscopy was used to assign the composition of each of the fractions; see the Supplemental Material [46] indicating that the amount of filled SWCNTs is negligible in the empty fraction ($< 3.7\%$), while in the PL spectra of the filled fraction a small contribution of empty SWCNTs can be observed, with an amplitude of $\sim 20\%$ of the total PL intensity. For temperature-dependent optical experiments, SWCNTs were drop cast on quartz substrates, dried, and mounted in a MicrostatHe2 cryostat (Oxford Instruments). The sample holder was in thermal contact with the heat exchanger and temperature sensor to allow for efficient temperature control. To avoid influences from intertube interactions such as energy transfer [60] and intertube exciton tunneling [61] on the PL spectra, the concentration of the SWCNTs in the films was kept sufficiently low. A continuous-wave Ti:sapphire laser operating at 822 nm was used to excite the (6,5) SWCNTs at their E_{11} phonon sidebands. For the wide-field imaging, the laser was expanded to a semihomogeneous spot of $\sim 60 \times 60$ μm and the excitation power was kept below 100 W/cm^2 in order to avoid any thermal effects. A 300 mm spectrograph equipped with a liquid-nitrogen-cooled InGaAs array detector was used to record the PL spectra and images.

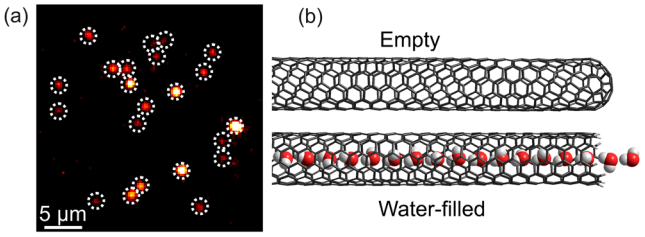

FIG. 1. (a) A representative wide-field PL image of DOC-wrapped empty (6,5) SWCNTs obtained at 4.2 K (localized exciton emission). The white circles mark individual SWCNTs. (b) Schematic molecular models of water-filled and empty (6,5) SWCNTs, demonstrating that the tube is just wide enough to fit a single linear chain of water molecules.

Figure 1(a) shows a representative wide-field PL image of DOC-wrapped empty (6,5) SWCNTs acquired at 4.2 K. Each white circle highlights an individual SWCNT. For each sample and at each temperature, a minimum of ten PL spectra were collected at different positions using the wide-field imaging method. Note that the so-obtained PL spectra are not from single tubes, but instead represent an ensemble average over a small area, effectively collecting PL signals from ~ 25 individual SWCNTs per spectrum. The samples were gradually cooled from room temperature to 4.2 K, and this was repeated for three separate samples for both the empty and the filled SWCNTs. Representative PL spectra of empty [Fig. 2(a)] and water-filled [Fig. 2(b)] SWCNTs at different temperatures are presented in Fig. 2. The E_{11} energy was obtained by fitting each of the spectra with a single Gaussian function. Figure 3(a) presents the mean E_{11} positions averaged over the ten different PL spectra obtained at each temperature, and additionally averaged over the three different samples. The error bars in Fig. 3(a) represent the standard error of the mean. The individual data sets for each sample can be found in the Supplemental Material [46].

Throughout the entire temperature range, the E_{11} energy of the water-filled SWCNTs is always smaller than that of the empty SWCNTs, which has previously been attributed to an increased dielectric screening for the water-filled SWCNTs [13,15,58]. Note also that the empty and water-filled SWCNT E_{11} energies observed for the film samples at room temperature are in excellent agreement with those reported for aqueous suspensions [15], proving that the SWCNTs remain well isolated from each other and from the substrate, and that the water remains encapsulated in the SWCNTs even under high vacuum conditions (possibly

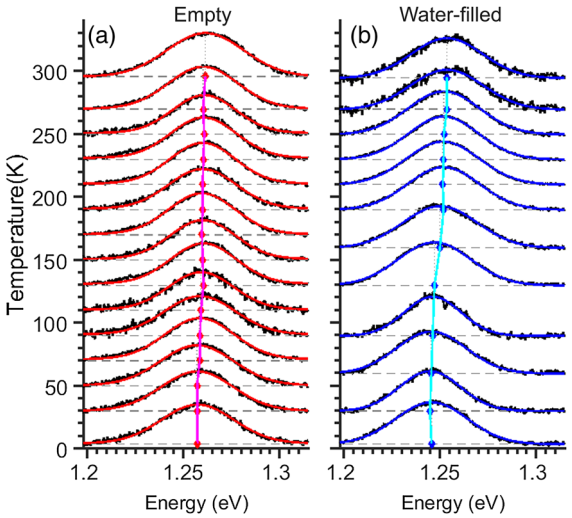

FIG. 2. Representative PL spectra of (a) empty and (b) water-filled SWCNTs at different temperatures. PL spectra are normalized and shifted vertically by the temperature they were measured at (indicated by the horizontal gray lines). Gaussian fits to the experimental data are presented in red (empty) and blue (filled). Peak positions of E_{11}, as obtained from the Gaussian fits, are marked as red and blue diamonds and connected with the peak of the curve by vertical dashed lines. Magenta and cyan lines connect the E_{11} points at different temperature.

due to the thick solid surfactant layer in which the SWCNTs are embedded). Also, the larger standard error of E_{11} due to tube-to-tube variations observed for the water-filled SWCNTs compared to that of the empty tubes is in excellent agreement with the internal-water-induced inhomogeneous spectral broadening observed in previous single-nanotube experiments [15].

To illustrate the temperature-induced shifts of the E_{11} peak positions observed for empty and water-filled SWCNTs, Fig. 3(b) presents the relative emission shifts using the value of E_{11} obtained at 4.2 K as the reference, i.e., $\Delta E_{11} = E_{11}(T) - E_{11}(4.2\ \mathrm{K})[\approx E_{11}(T) - E_{11}(0\ \mathrm{K})]$. The E_{11} peak position of the empty SWCNTs blueshifts linearly with increasing temperature at a slope of $9.7 \pm 1.7 \times 10^{-3}$ meV, resulting in an overall shift of only 2.8 meV over the entire temperature range (4.2–296 K).

These temperature-dependent PL shifts can be ascribed to two competing effects. First of all, softening of the strong coupling between band-edge states and the lowest energy optical phonon modes results in a redshift of E_{11} for all SWCNT chiralities at increasing temperatures [62–64] (observed for strain-free suspended tubes [62]; note that this shift is opposite from what we observe). Additionally, previous studies demonstrated that due to the mismatch of the thermal expansion coefficients of SWCNTs and their host matrices, the emission energy can either blue- or redshift depending on the chirality [62,64–68], and in fact, this strain-induced shift dominates in surfactant-coated SWCNTs [64,65,67]. Following a similar procedure as

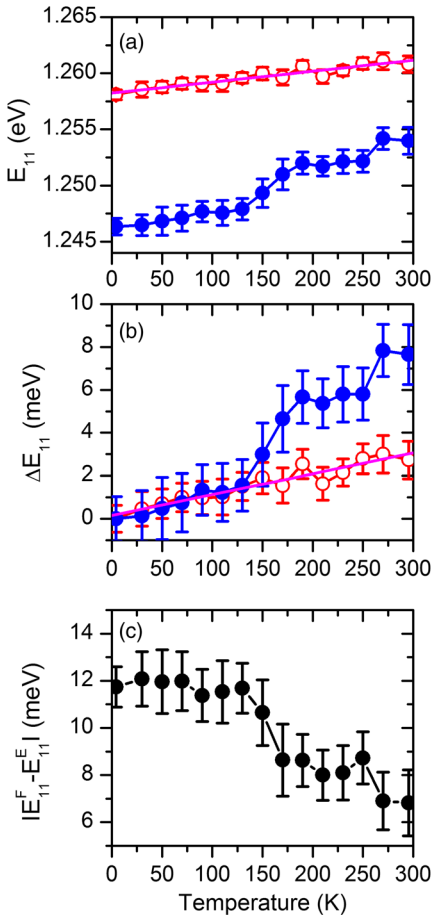

FIG. 3. (a) Mean PL peak positions (E_{11}) and standard errors of the mean for the empty (red, open circles) and water-filled (blue, filled circles) SWCNTs measured at different temperatures. The mean values and standard errors of the mean were determined from wide-field PL spectra measured for three different samples, with at least ten different positions for each sample at each temperature. The values of the empty SWCNTs are fitted linearly (magenta). (b) $\Delta E_{11} = E_{11}(T) - E_{11}(4.2\ \mathrm{K})$ for empty and water-filled SWCNTs. The values of the empty SWCNTs are fitted linearly (magenta). (c) Energy difference for water-filled and empty SWCNTs ($|E^F_{11} - E^E_{11}|$) as a function of temperature.

defined previously in the literature for SWCNTs embedded in surfactants or polymers [64,65,67], a uniaxial strain component of $(0.044 \pm 0.004) \times 10^{-3}\%/\mathrm{K}$ is exerted by the external host environment on the empty SWCNTs (see the Supplemental Material [46]).

Superimposed on the linear temperature-dependent PL shifts observed for the empty SWCNTs [Fig. 3(b)], an additional stepwise PL shift is observed for the water-filled SWCNTs centered at ~150 K. Such a change has previously been observed in FTIR measurements for larger-diameter mixed-chirality SWCNTs embedded in films [68], and was postulated to arise either from adsorption or desorption of molecules on the external SWCNT surface or from a phase transition of water inside the SWCNTs. However, the results remained inconclusive on the true origin.

In this work, however, the empty SWCNTs can serve as an ideal reference system, allowing us to assign this change in slope for the water-filled SWCNTs to temperature-induced changes occurring in the chain of water molecules encapsulated inside the (6,5) SWCNTs. Subtracting the data of the empty SWCNTs from those of the water-filled SWCNTs (denoted as $|E_{11}^F - E_{11}^E|$) allows us to exclude the effect of the external host matrix (i.e., the surfactant layer). Therefore, $|E_{11}^F - E_{11}^E|$ represents the sole effect of the encapsulated water molecules on the electronic transition energies of SWCNTs, which clearly defines a sudden transition centered at ~150 K.

The change of E_{11} observed at ~150 K is a sizeable fraction of the maximal difference in E_{11} between empty and water-filled SWCNTs, and more than 2 times larger than the strain-induced shift observed for the empty SWCNTs imposed by the external environment over the entire temperature range. Therefore, it is unlikely that the additional PL shift of the water-filled SWCNTs at ~150 K is mediated through strain from the encapsulated molecules (note that the diameter of the (6,5) SWCNTs is sufficiently large to provide more than enough space for the single file water molecules [30], see also Fig. 1). Theoretical calculations [69] and experimental studies [16,69] have suggested that optical transition energies of SWCNTs are extremely sensitive to both the effective size and orientation of the molecular dipoles encapsulated in or adsorbed on SWCNTs (larger effect for dipoles oriented perpendicular to the tube axis [69]). Therefore, a significant change in the orientation of the water dipoles most likely lies at the origin of the observed spectral shift.

Inspired by this peculiar experimental observation, and furthermore motivated by the fact that theoretical calculations have predicted qualitatively different ground state structures for 1D water chains in nanochannels [14,30, 38–40], it seemed plausible that quasiphase transitions might occur between such differently ordered water structures. To assess whether significant changes in dipole orientations indeed occur in the relevant temperature range, we performed MD simulations of a single-file chain of water molecules in a (6,5) SWCNT as a function of temperature, using the Chemistry at Harvard Macromolecular Mechanics (CHARMM) force field [70] combined with realistic partial atomic charges for the water molecules (see the Supplemental Material [46]). Figure 4 presents the angular distribution of water dipole moments relative to the SWCNT axis, for a few selected temperatures (see also Figs. S7–S8 in the Supplemental Material [46]). At low temperature, the water molecules form a traditional hydrogen-bonded chain with ferroelectrically ordered water dipoles pointing at angles of $\theta \sim 31°$ with the SWCNT axis (dipole moment components parallel to the tube axis all aligned in the same sense; perpendicular components aligned in alternating senses, see also Fig. S9 in the Supplemental Material [46]). Around ~70 K, dipole orientations parallel to the tube axis ($\theta \sim 0°$) start to dominate, corresponding to the occurrence of bifurcated hydrogen bonds (i.e., hydrogen bond from a single oxygen atom distributed over both hydrogen atoms of a single neighboring water molecule). For $T > 200$ K also angles of 90° start to occur frequently, allowing the dipole moments to flip their orientation completely, and destroying the ferroelectric order. The MD calculations thus indicate three different regimes (hence two transitions): classical hydrogen-bonded, predominantly bifurcated hydrogen-bonded, and disordered chains. The direction of the experimentally observed shift is both in line with the much larger effective total dipole moment (albeit along the SWCNT axis) of the ferroelectrically ordered chains (both classical and bifurcated hydrogen bonds) with respect to a disordered chain [Fig. S8(b) in the Supplemental Material [46]], and with the increased angle of the dipoles with the SWCNT axis for the classical hydrogen-bonded chain with respect to the predominantly bifurcated state. Thus, the MD calculations support the interpretation that changes in the dipole orientation are at the basis of the observed change in transition energy of the SWCNTs, but further, more extended theory is certainly desired to identify the exact nature of this quasiphase transition.

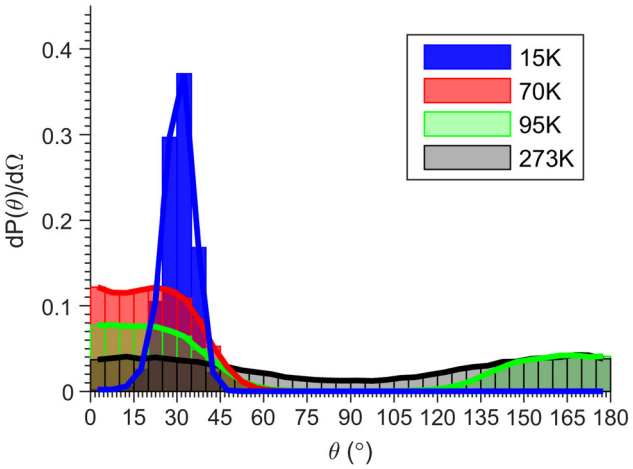

FIG. 4. Orientational probability distribution $P(\theta)$ per solid angle ($d\Omega$) of the water dipoles relative to the nanotube axis for different temperatures, using the contributions from the central seven (of the total 11) water molecules in the MD simulation (see also the Supplemental Material [46]).

In conclusion, our experimental results provide new insights into the phase behavior of water molecules confined to a single file inside SWCNTs and demonstrate the need for more advanced theories to explain the origin of the experimentally observed transition. With the electronic transition energies of SWCNTs acting as very sensitive sensors for the encapsulated molecules, PL spectroscopy opens new perspectives to investigate the temperature-dependent behavior of confined molecules. SWCNTs present a close analogy with many natural nanopore systems and thus can serve as general model systems for understanding the behavior of

water molecules in more complex natural systems [11,12]. The superior water molecule permeability of carbon nanotubes has enabled their applications in highly efficient purification and desalination devices [5–7,9,22–25] and the study of ultrafast proton transport through one-dimensional molecular arrays [2,3,8]. Our finding of a confined water phase transition in SWCNTs is essential to understand and achieve the fundamental limits of carbon nanotube nanofluidics devices.

This work was supported in part by the LANL LDRD program and was performed in part at the Center for Integrated Nanotechnologies, a U.S. Department of Energy, Office of Science User Facility. S. C. and W. W. acknowledge financial support from the Fund for Scientific Research Flanders, Belgium (FWO, Projects No. G040011N, No. G021112N, No. 1513513N, and No. 1512716N), which also supported S. C. through a postdoctoral fellowship and a mobility grant for visiting LANL. Funding from the Hercules Foundation (Grant No. AUHA/13006) and the European Research Council (ERC) under Horizon 2020/ERC starting Grant Agreement No. 679841 is gratefully acknowledged.

X. M. and S. C. contributed equally to this work.

*Corresponding authors.
xuedan.ma@anl.gov
†sofie.cambre@uantwerpen.be
‡Present address: Center for Nanoscale Materials, Argonne National Laboratory, Lemont, Illinois 60439, USA.

[1] I. Brovchenko and A. Oleinikova, *Interfacial and Confined water* (Elsevier, New York, 2008).
[2] P. Agre and D. Kozone, Aquaporin water channels: Molecular mechanisms for human diseases, FEBS Lett. **555**, 72 (2003).
[3] J. C. Rasaiah, S. Garde, and G. Hummer, Water in nonpolar confinement: From nanotubes to proteins and beyond, Annu. Rev. Phys. Chem. **59**, 713 (2008).
[4] G. Hummer, J. C. Rasaiah, and J. P. Noworyta, Water conduction through the hydrophobic channel of a carbon nanotube, Nature (London) **414**, 188 (2001).
[5] J. K. Holt, H. G. Park, Y. Wang, M. Stadermann, A. B. Artyukhin, C. P. Grigoropoulos, A. Noy, and O. Bakajin, Fast mass transport through sub-2-nanometer carbon nanotubes, Science **312**, 1034 (2006).
[6] W. Sparreboom, A. van den Berg, and J. C. T. Eijkel, Principles and applications of nanofluidic transport, Nat. Nanotechnol. **4**, 713 (2009).
[7] A. Noy, H. G. Park, F. Fornasiero, J. K. Holt, C. P. Grigoropoulos, and O. Bakajin, Nanofluidics in carbon nanotubes, Nano Today **2**, 22 (2007).
[8] R. H. Tunuguntla, F. I. Allen, K. Kim, A. Belliveau, and A. Noy, Ultrafast proton transport in sub-1-nm diameter carbon nanotube porins, Nat. Nanotechnol. **11**, 639 (2016).
[9] B. Corry, Designing carbon nanotube membranes for efficient water desalination, J. Phys. Chem. B **112**, 1427 (2008).
[10] A. Jorio, M. S. Dresselhaus, and G. Dresselhaus, *Carbon Nanotubes: Advanced Topics in the Synthesis, Structure, Properties and Applications* (Springer, New York, 2008).
[11] J. K. Holt, Methods for probing water at the nanoscale, Microfluid. Nanofluid. **5**, 425 (2008).
[12] A. Berezhkovskii and G. Hummer, Single-File Transport of Water Molecules through a Carbon Nanotube, Phys. Rev. Lett. **89**, 064503 (2002).
[13] W. Wenseleers, S. Cambré, J. Čulin, A. Bouwen, and E. Goovaerts, Effect of water filling on the electronic and vibrational resonances of carbon nanotubes: Characterizing tube opening by Raman spectroscopy, Adv. Mater. **19**, 2274 (2007).
[14] S. Cambré, B. Schoeters, S. Luyckx, E. Goovaerts, and W. Wenseleers, Experimental Observation of Single-File Water Filling of Thin Single-Wall Carbon Nanotubes Down to Chiral Index (5,3), Phys. Rev. Lett. **104**, 207401 (2010).
[15] S. Cambré, S. M. Santos, W. Wenseleers, A. R. T. Nugraha, R. Saito, L. Cognet, and B. Lounis, Luminescence properties of individual empty and water-filled single-walled carbon nanotubes, ACS Nano **6**, 2649 (2012).
[16] S. Cambré, J. Campo, C. Beirnaert, C. Verlackt, P. Cool, and W. Wenseleers, Asymmetric dyes align inside carbon nanotubes to yield a large nonlinear optical response, Nat. Nanotechnol. **10**, 248 (2015).
[17] J. Campo, Y. Piao, S. Lam, C. M. Stafford, J. K. Streit, J. R. Simpson, A. R. Hight Walker, and J. A. Fagan, Enhancing single-wall carbon nanotube properties through controlled endohedral filling, Nanoscale Horiz. **1**, 317 (2016).
[18] T. Takenobu, T. Takano, M. Shiraishi, Y. Murakami, M. Ata, H. Kataura, Y. Achiba, and Y. Iwasa, Stable and controlled amphoteric doping by encapsulation of organic molecules inside carbon nanotubes, Nat. Mater. **2**, 683 (2003).
[19] K. Yanagi, K. Iakoubovskii, H. Matsui, H. Matsuzaki, H. Okamoto, Y. Miyata, Y. Maniwa, S. Kazaoui, N. Minami, and H. Kataura, Photosensitive function of encapsulated dye in carbon nanotubes, J. Am. Chem. Soc. **129**, 4992 (2007).
[20] E. Gaufrès, N. Y. W. Tang, F. Lapointe, J. Cabana, M. A. Nadon, N. Cottenye, F. Raymond, T. Szkopek, and R. Martel, Giant Raman scattering from J-aggregated dyes inside carbon nanotubes for multispectral imaging, Nat. Photonics **8**, 72 (2014).
[21] K. Yanagi, Y. Miyata, and H. Kataura, Highly stabilized β-Carotene in carbon nanotubes, Adv. Mater. **18**, 437 (2006).
[22] B. Lee, Y. Baek, M. Lee, D. H. Jeong, H. H. Lee, J. Yoon, and Y. H. Kim, A carbon nanotube wall membrane for water treatment, Nat. Commun. **6**, 7109 (2015).
[23] E. Secchi, S. Marbach, A. Nigus, D. Stein, A. Siria, and L. Bocquet, Massive radius-dependent flow slippage in carbon nanotubes, Nature (London) **537**, 210 (2016).
[24] M. Elimelech and W. A. Phillip, The future of seawater desalination: Energy, technology, and the environment, Science **333**, 712 (2011).
[25] R. Das, M. E. Ali, S. B. A. Hamid, S. Ramakrishna, and Z. Z. Chowdhury, Carbon nanotube membranes for water purification: A bright future in water desalination, Desalination **336**, 97 (2014).
[26] K. Koga, G. T. Gao, H. Tanaka, and X. C. Zeng, Formation of ordered ice nanotubes inside carbon nanotubes, Nature (London) **412**, 802 (2001).
[27] E. Paineau, P.-A. Albouy, S. Rouzière, A. Orecchini, S. Rols, and P. Launois, X-ray scattering determination of the

structure of water during carbon nanotube filling, Nano Lett. **13**, 1751 (2013).
[28] S. Chiashi, T. Hanashima, R. Mitobe, K. Nagatsu, T. Yamamoto, and Y. Homma, Water encapsulation control in individual single-walled carbon nanotubes by laser irradiation, J. Chem. Phys. Lett. **5**, 408 (2014).
[29] E. Ising, Beitrag zur Theorie des Ferromagnetismus, Z. Phys. **31**, 253 (1925).
[30] J. Wang, Y. Zhu, J. Zhou, and X.-H. Lu, Diameter and helicity effects on static properties of water molecules confined in carbon nanotubes, Phys. Chem. Chem. Phys. **6**, 829 (2004).
[31] D. Takaiwa, I. Hatano, K. Koga, and H. Tanaka, Phase diagram of water in carbon nanotubes, Proc. Natl. Acad. Sci. U.S.A. **105**, 39 (2008).
[32] Y. Maniwa, H. Kataura, M. Abe, S. Suzuki, Y. Achiba, H. Kira, and K. Matsuda, Phase transition in confined water inside carbon nanotubes, J. Phys. Soc. Jpn. **71**, 2863 (2002).
[33] H. Kyakuno, K. Matsuda, H. Yahiro, Y. Inami, T. Fukuoka, Y. Miyata, K. Yanagi, Y. Maniwa, H. Kataura, T. Saito, M. Yumura, and S. Iijima, Confined water inside single-walled carbon nanotubes: Global phase diagram and effect of finite length, J. Chem. Phys. **134**, 244501 (2011).
[34] O. Byl, J.-C. Liu, Y. Wang, W.-L. Yim, J. K. Johnson, and J. T. Yates, Unusual hydrogen bonding in water-filled carbon nanotubes, J. Am. Chem. Soc. **128**, 12090 (2006).
[35] S. Dalla Bernardina, E. Paineau, J.-B. Brubach, P. Judeinstein, S. Rouzière, P. Launois, and P. Roy, Water in carbon nanotubes: The peculiar hydrogen bond network revealed by infrared spectroscopy, J. Am. Chem. Soc. **138**, 10437 (2016).
[36] A. I. Kolesnikov, J.-M. Zanotti, C.-K. Loong, P. Thiyagarajan, A. P. Moravsky, R. O. Loutfy, and C. J. Burnham, Anomalously Soft Dynamics of Water in a Nanotube: A Revelation of Nanoscale Confinement, Phys. Rev. Lett. **93**, 035503 (2004).
[37] K. Matsuda, T. Hibi, H. Kadowaki, H. Kataura, and Y. Maniwa, Water dynamics inside single-wall carbon nanotubes: NMR observations, Phys. Rev. B **74**, 073415 (2006).
[38] A. Alexiadis and S. Kassinos, Molecular simulation of water in carbon nanotubes, Chem. Rev. **108**, 5014 (2008).
[39] J. Köfinger, G. Hummer, and C. Dellago, Single-file water in nanopores, Phys. Chem. Chem. Phys. **13**, 15403 (2011).
[40] Y. Bushuev, S. Davletbaeva, and F. F. Muguet, Hydration simulations of a carbon nanotube, immersed in water, according to the 3-attractor water model, Sensors **5**, 139 (2005).
[41] V. V. Chaban and O. V. Prezhdo, Water boiling inside carbon nanotubes: Toward efficient drug release, ACS Nano **5**, 5647 (2011).
[42] C. Y. Khripin, J. A. Fagan, and M. Zheng, Spontaneous partition of carbon nanotubes in polymer-modified aqueous phases, J. Am. Chem. Soc. **135**, 6822 (2013).
[43] N. K. Subbaiyan, S. Cambré, A. N. Parra-Vasquez, E. H. Haroz, S. K. Doorn, and J. G. Duque, Role of surfactants and salt in aqueous two-phase separation of carbon nanotubes toward simple chirality isolation, ACS Nano **8**, 1619 (2014).
[44] N. K. Subbaiyan, A. N. G. Parra-Vasquez, S. Cambré, M. Santiago Cordoba, S. Ebru Yalcin, C. E. Hamilton, N. Mack, J. Blackburn, S. K. Doorn, and J. G. Duque, Bench-top aqueous two-phase extraction of isolated individual single-walled carbon nanotubes, Nano Res. **8**, 1755 (2015).
[45] S. M. Bachilo, M. S. Strano, C. Kittrell, R. H. Hauge, R. E. Smalley, and R. B. Weisman, Structure-assigned optical spectra of single-walled carbon nanotubes, Science **298**, 2361 (2002).
[46] See Supplemental Material at http://link.aps.org/supplemental/10.1103/PhysRevLett.118.027402, which includes Refs. [47–56], for spectroscopic sample characterization, all temperature-dependent PL spectra, and more details on the MD simulations.
[47] L. Vinna, S. Logothetidis, and M. Cardona, Temperature dependence of the dielectric function of germanium, Phys. Rev. B **30**, 1979 (1984).
[48] L. Yang and J. Han, Electronic Structure of Deformed Carbon Nanotubes, Phys. Rev. Lett. **85**, 154 (2000).
[49] M. Huang, Y. Wu, B. Chandra, H. Yan, Y. Shan, T. F. Heinz, and J. Hone, Direct Measurement of Strain-Induced Changes in the Band Structure of Carbon Nanotubes, Phys. Rev. Lett. **100**, 136803 (2008).
[50] J. W. Ding, X. H. Yan, and J. X. Cao, Analytical relation of band gaps to both chirality and diameter of single-wall carbon nanotubes, Phys. Rev. B **66**, 073401 (2002).
[51] S. Reich, J. Maultzsch, C. Thomsen, and P. Ordejón, Tight-binding description of graphene, Phys. Rev. B **66**, 035412 (2002).
[52] J. Cao, Q. Wang, and H. Dai, Electromechanical Properties of Metallic, Quasimetallic, and Semiconducting Carbon Nanotubes under Stretching, Phys. Rev. Lett. **90**, 157601 (2003).
[53] V. Perebeinos, J. Tersoff, and P. Avouris, Scaling of Excitons in Carbon Nanotubes, Phys. Rev. Lett. **92**, 257402 (2004).
[54] W. L. Jorgensen, J. Chandrasekhar, J. D. Madura, R. W. Impey, and M. L. Klein, Comparison of simple potential functions for simulating liquid water, J. Chem. Phys. **79**, 926 (1983).
[55] D. J. Mann and M. D. Halls, Water Alignment and Proton Conduction inside Carbon Nanotubes, Phys. Rev. Lett. **90**, 195503 (2003).
[56] J. J. P. Stuart, Optimization of parameters for semiempirical methods V: Modification of NDDO approximations and application to 70 elements, J. Mol. Model. **13**, 1173 (2007).
[57] W. Wenseleers, I. I. Vlasov, E. Goovaerts, E. D. Obraztsova, A. S. Lobach, and A. Bouwen, Efficient isolation and solubilization of pristine single-walled nanotubes in Bile salt micelles, Adv. Funct. Mater. **14**, 1105 (2004).
[58] S. Cambré and W. Wenseleers, Separation and diameter-sorting of empty (end-capped) and water-filled (open) carbon nanotubes by density gradient ultracentrifugation, Angew. Chem., Int. Ed. **50**, 2764 (2011).
[59] S. Cambré, P. Muyshondt, M. Federicci, and W. Wenseleers, Chirality-dependent densities of carbon nanotubes by in situ 2D fluorescence-excitation and Raman characterisation in a density gradient after ultracentrifugation, Nanoscale **7**, 20015 (2015).
[60] H. Qian, P. T. Araujo, C. Georgi, T. Gokus, N. Hartmann, A. A. Green, A. Jorio, M. C. Hersam, L. Novotny, and A. Hartschuh, Visualizing the local optical response of semiconducting carbon nanotubes to DNA-wrapping, Nano Lett. **8**, 2706 (2008).

[61] R. D. Mehlenbacher, M.-Y. Wu, M. Grechko, J. E. Laaser, M. S. Arnold, and M. T. Zanni, Photoexcitation dynamics of coupled semiconducting carbon nanotube thin films, Nano Lett. **13**, 1495 (2013).

[62] S. B. Cronin, Y. Yin, A. Walsh, R. B. Capaz, A. Stolyarov, P. Tangney, M. L. Cohen, S. G. Louie, A. K. Swan, M. S. Unlu, B. B. Goldberg, and M. Tinkham, Temperature Dependence of the Optical Transition Energies of Carbon Nanotubes: The Role of Electron-Phonon Coupling and Thermal Expansion, Phys. Rev. Lett. **96**, 127403 (2006).

[63] R. B. Capaz, C. D. Spataru, P. Tangney, M. L. Cohen, and S. G. Louie, Temperature Dependence of the Band Gap of Semiconducting Carbon Nanotubes, Phys. Rev. Lett. **94**, 036801 (2005).

[64] D. Karaiskaj, C. Engtrakul, T. McDonald, M. J. Heben, and A. Mascarenhas, Intrinsic and Extrinsic Effects in the Temperature-Dependent Photoluminescence of Semiconducting Carbon Nanotubes, Phys. Rev. Lett. **96**, 106805 (2006).

[65] K. Arnold, S. Lebedkin, O. Kiowski, F. Hennrich, and M. M. Kappes, Matrix-Imposed stress-induced shifts in the photoluminescence of single-walled carbon nanotubes at low temperatures, Nano Lett. **4**, 2349 (2004).

[66] L.-J. Li, R. J. Nicholas, R. S. Deacon, and P. A. Shields, Chirality Assignment of Single-Walled Carbon Nanotubes with Strain, Phys. Rev. Lett. **93**, 156104 (2004).

[67] C. Li and T.-W. Chou, Axial and radial thermal expansions of single-walled carbon nanotubes, Phys. Rev. B **71**, 235414 (2005).

[68] A. Siitonen, H. Kunttu, and M. Pettersson, Temperature dependence of electronic transitions of single-wall carbon nanotubes: Observation of an abrupt blueshift in near-infrared absorption, J. Phys. Chem. C **111**, 1888 (2007).

[69] E. Malic, C. Weber, M. Richter, V. Atalla, T. Klamroth, P. Saalfrank, S. Reich, and A. Knorr, Microscopic Model of the Optical Absorption of Carbon Nanotubes Functionalized with Molecular Spiropyran Photoswitches, Phys. Rev. Lett. **106**, 097401 (2011).

[70] B. R. Brooks, R. E. Bruccoleri, B. D. Olafson, D. J. States, S. Swaminathan, and M. Karplus, CHARMM: A program for macromolecular energy, minimization, and dynamics calculations, J. Comput. Chem. **4**, 187 (1983).